Current Research in Food Science 5 (2022) 1243–1250

Contents lists available at ScienceDirect

Current Research in Food Science

journal homepage: www.sciencedirect.com/journal/current-research-in-food-science

Effects and mechanism of natural phenolic acids/fatty acids on copigmentation of purple sweet potato anthocyanins

Xiaorui Lv [a], Jianlou Mu [a], Wenxiu Wang [a], Yaqiong Liu [a], Xiaomin Lu [b], Jianfeng Sun [a,**], Jie Wang [a], Qianyun Ma [a,*]

[a] College of Food Science and Technology, Hebei Agricultural University, Baoding, 071000, China
[b] Department of Forest Biomaterials, North Carolina State University, Raleigh, NC, 27695, USA

ARTICLE INFO

Handling editor: Professor Aiqian Ye

Keywords:
Anthocyanin
Copigmentation
Bathochromic shift
Hyperchromic effect
Quantum mechanic

ABSTRACT

Anthocyanins are attractive alternatives to colorants; however, their low color stability hinders practical application. Copigmentation can enhance both the color intensity and color stability of complexes. Herein, we report an investigation of copigmentation reactions between purple sweet potato anthocyanins (PSA1) and phenolic acids (tannic, ferulic, and caffeic acids) or fatty acids (tartaric and malic acids) at pH 3.5. The effects of the mole ratios of the copigment and the reaction temperature were examined. In addition, quantum mechanical computations were performed to investigate molecular interactions. The optimum PSA:copigment molar ratio was found to be 1:100. The strongest bathochromic and hyperchromic effects were observed for copigmentation with tannic acid (Tan), which might be attributable to the fact that its HOMO-LUMO energy gap was the smallest among the investigated copigments, and because it has a greater number of phenolic aromatic and groups to form more van der Waals and hydrogen bond interactions. However, the formation of the PSA-caffeic acid (Caf) complex was accompanied by the greatest drop in enthalpy (−33.18 kJ/mol) and entropy (−74.55 kJ/mol), and this was the most stable complex at 90 °C. Quantum mechanical calculations indicated that hydrogen bonds and van der Waals force interactions contributed to the color intensification effect of copigmentation. These findings represent an advancement in our understanding of the properties of PSA, expanding the application scope of this natural product.

1. Introduction

Color is crucial for attracting the attention of consumers, especially for the sale of foods, clothes, and decorative items. Synthetic colorants have been used in food for a few years. However, excessive use of some synthetic dyes can lead to renal failure, hepatocellular damage, and angioedema (Xu et al., 2022). For example, Brilliant Blue FCF and Green S can cause hyperactivity and even carcinogenic pathologies in children (Silva et al., 2022). In addition, Tartrazine, Azorubine, and Allura Red bind to human serum albumin decreased the transport functions of proteins (Amchova et al., 2015). Therefore, there is an urgent need for healthy non-toxic natural colorants. It is estimated that global revenues from natural colorants will reach $1620 million by 2023 (Wu et al., 2022).

Anthocyanins impart colors in the orange-red-blue spectrum to flowers, vegetables, and fruits, and these are the most important class of natural pigments (Alara et al., 2021). They have been widely used in foods because of their excellent water solubility and bright tones. Anthocyanins also possess antioxidant and other biological activities (Zheng et al., 2021). Indeed, they have been shown to reduce the risk of diabetes (Tsuda, 2016), neuronal diseases (Winter and Bickford, 2019), and obesity (Choi et al., 2020). Despite such advantages, these anthocyanins are easily degraded by variations in temperature, illumination, and oxygen levels, which restricts their further adoption as alternatives to synthetic colorants. So far, four main mechanisms for stabilizing anthocyanins have been proposed: copigmentation, biosynthesis,

Abbreviations: PSA, purple sweet potato anthocyanins; Tan, tannic acid; Caf, caffeic acid; Fer, ferulic acid; Tar, tartaric acid; Mal, malic acid; PCG, petunidin-3-coumaroylrutinoside-5-glucoside; DFT, density functional theory; IGM, independent gradient model; BCPs, bond critical point; HBs, hydrogen bond; vdWs, van der Waals; RCPs, ring citica points; CCPs, cage critical points.

* Corresponding author.
** Corresponding author.
E-mail addresses: causunjf@hebau.edu.cn (J. Sun), mqy26@hebau.edu.cn (Q. Ma).

https://doi.org/10.1016/j.crfs.2022.08.003
Received 14 May 2022; Received in revised form 4 August 2022; Accepted 6 August 2022
Available online 13 August 2022

encapsulation, and acylation. Reported copigmentation reactions involved the formation of complexes of anthocyanins and copigments based on noncovalent interactions, and these may protect the anthocyanin molecule from nucleophilic attack by water (Gençdağ et al., 2022). Compared with other methods, copigmentation not only offers improved anthocyanin stability but also enhanced color intensity (Cai et al., 2022). Increased color (absorption) intensity is extremely important for colorants to make food appear attractive color with less addition of colorants. Additionally, copigmentation strengthens the antioxidant properties of anthocyanins (Yang et al., 2021). Commonly used copigments include organic acids, alkaloids, polysaccharides, flavonoids, and proteins (Fan et al., 2019). The acids used are typically divided into two groups: aromatic acids and fatty acids (Aleixandre-Tudó et al., 2013). The type and number of ligands linked to the benzene ring in a phenolic acid structure has a direct impact on copigmentation. Indeed, it is known that π-π interactions, the driving force of copigmentation, can occur between the phenolic benzene ring and anthocyanins, or between hydroxy and carbonyl O groups. Hence, the number of hydroxy groups in a fatty acid also has a direct effect on its copigmentation capacity. In addition, it was reported that acylated anthocyanins have higher stability when copigmented with acids (Fenger et al., 2021). However, the effects of phenolic acids and fatty acids copigmentation on acylated anthocyanins are not detailed or compared in depth.

Purple sweet potato contains large amounts of acylated anthocyanins and phenolic compounds (Huang et al., 2021) and is the staple food in many developing countries because of its high productivity but low input requirements (Su et al., 2019). It was reported that PSA have higher color intensity than anthocyanins from other plant sources, such as perilla, strawberries, and red cabbage (He et al., 2015). Therefore, in order to further investigate the effects of different types of organic acids on acylated anthocyanins, we chose PSA. Moreover, in line with the high degree of safety of PSA, natural phenolic acids such as Tan, ferulic acid (Fer), Caf, and fatty acids such as tartaric acid (Tar), and malic acid (Mal) were selected; the structures of these are shown in Fig. 1. We first analyzed the structures and electron density distributions of these organic acids, and then studied the effect of the PSA-to-copigment molar ratio for the five natural aromatic and fatty acids copigments on the PSA color. Subsequently, the effects of the heating temperature on the copigmentation interactions were investigated, and possible mechanisms involved in the complexation process were studied using quantum mechanical calculations. The results of this study will help to promote the application of PSA as a natural colorant in the food industry. Furthermore, we believe that our conclusions add vital fundamental scientific data to the literature related to the copigmentation of phenolic and fatty acids with PSA.

2. Materials and methods

2.1. Materials

Purple sweet potatoes were provided by Zhangjiakou Hongji Industry Group Co., Ltd (Heibei, China). Chromatography-grade formic acid and acetonitrile were obtained from Mreda Co., Ltd (Beijing, China). Tan, Fer, Caf, Tar, Mal, and dimethyl sulfoxide were purchased from Yuanye Bio-Technology Co., Ltd (Shanghai, China). All other materials were purchased from Sinopharm Chemical Reagent Co., Ltd (Shanghai, China).

2.2. Anthocyanin extraction and structural analysis

PSA was obtained using a previously reported method (Liu et al., 2021), with several modifications. Washed potatoes chopped into approximately 2 cm slices, freeze-dried (FD-1C-50, Beijing Boyikang Instrument Co., Ltd., Beijing, China) and crushed into powder (80-mesh), followed by dissolution in 80% ethanol solution and

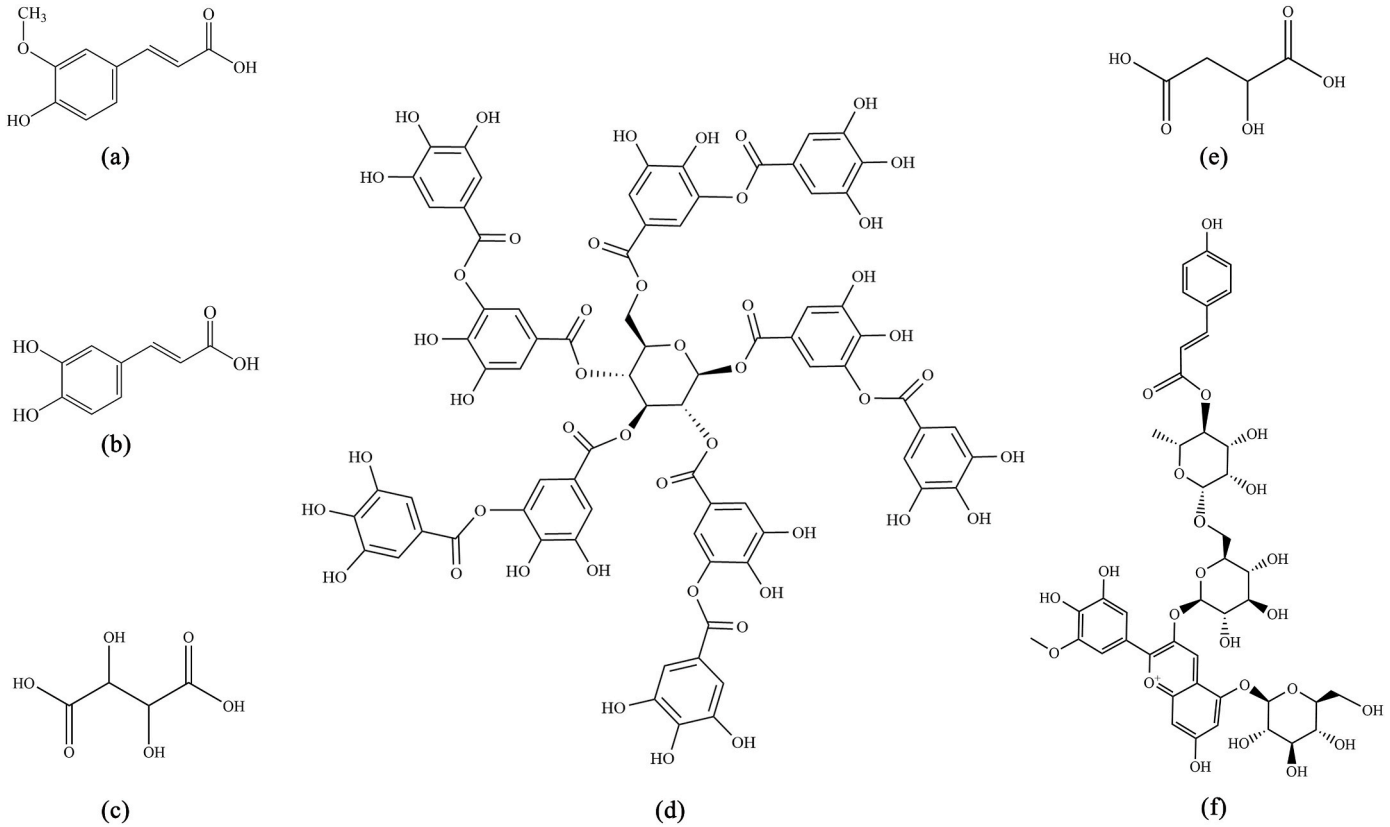

Fig. 1. Structure of the organic acids used as copigments in this study: (a) Fer, (b) Caf, (c) Tar, (d) Tan, (e) Mal, and (f) PCG.

ultrasonication for 40 min at 25 °C (SB-5200 DTD, Scientz Instrument Co., Ltd, Ningbo, China). The solution was extracted in the dark for 24 h. The extract solution was concentrated through rotary evaporation at 40 ± 2 °C (RE52cs, Shanghai Yarong biochemical Co., Ltd., Shanghai, China), followed by purification using an HP-20 macroporous resin column. Finally, the sample was rotary-evaporated and vacuum freeze-dried at −40 ± 1 °C for 48 h using a freeze-dryer, to obtain the PSA powder. The total anthocyanin content of PSA was determined by the pH differential method (He et al., 2016).

2.3. UHPLC-MS

The main components of anthocyanins in the PSA sample were identified using a Thermo Scientific Vanquish Duo ultra-high-performance liquid chromatography (UHPLC) system, a Q-Exactive HF mass spectrometer, and a Zorbax Eclipse C18 (1.8 μm, 2.1 × 100 mm). The mobile phase was a mixture of (A) water and (B) acetonitrile with a gradient-elution rate of 300 μL min^{-1}. The composition of the mobile phase varied as follows: 0–5 min, isocratic condition, 2% B; 2–20 min, 98% B; 20–25 min, 2% B; 23–30 min, isocratic condition, 2% B. The temperature of the drying gas in the ionization source was 300 °C. The mass spectrometry parameters were as follows: source type, high energy collision dissociation; dry gas flow, 45 mL/min; scan range, 70–1050 m/z; capillary voltage, 3.0 kV.

2.4. Preparation and temperature treatment of anthocyanin−copigment complexes

The experimental solution was prepared according to the method reported by Babaloo and Jamei (2018). Anthocyanins were dissolved in 0.5% trifluoroacetic acid, while the copigments were dissolved in 10% DMSO with 0.02 M ammonium acetate. The pH of copigmentation was regulated to 3.5 ± 0.02.

Anthocyanins were mixed with copigment solutions in molar ratios of 1:10, 1:50, 1:100, and 1:150. These solutions were incubated at room temperature for 30 min in the dark. Their absorption spectra were recorded using a UV–visible spectrophotometer (α-1500, Shanghai, China) in the visible range (400–700 nm). The enhancement of the color intensity of anthocyanins owing to their intermolecular copigmentation with organic acids was studied in terms of spectrometric parameters, such as the hyperchromic effect ($\Delta A_{max} = \frac{A-A_0}{A_0}$) and bathochromic shift ($\Delta\lambda_{max} = \lambda - \lambda_0$).

2.5. Determination of thermodynamic parameters

The effect of temperature (30, 40, 60, 80, and 90 °C) on the copigmentation reactions was evaluated using identical molar ratios (1:100) of each copigment. The values of the equilibrium constant (K), Gibbs free energy (ΔG^o), enthalpy change (ΔH^o), and entropy change (ΔS^o) for the intermolecular interaction process were determined using the following equations:

$$ln\left(\frac{A-A_0}{A_0}\right) = lnK + nln[C_p]_0 \quad (1)$$

$$\Delta G^o = -RT \times lnK \quad (2)$$

$$\Delta G^o = \Delta H^o - T\Delta S^o \quad (3)$$

$$ln\left(\frac{A-A_0}{A_0}\right) = -\frac{\Delta H^o}{RT} + \frac{\Delta S^o}{R} + nln[C_p]_0 \quad (4)$$

Here, A is the absorbance of the anthocyanin extracts including organic acids (at λ_{max}), A_0 is the absorbance of the control sample at 30 °C (at λ_{max}), parameter n is the stoichiometric ratio between anthocyanins and copigments in the complexes, $[C_P]_0$ represents the copigment concentration, R is the global gas constant (8.314 J/mol·K), and T is the temperature in Kelvin.

2.6. Quantum mechanics calculations

The conformation of petunidin-3-coumaroylrutinoside-5-glucoside (PCG) and Fer were confirmed using the Molclus progam (Lu, 2021). All the complexes obtained were pre-optimized using the semi-empirical B3LYP-D3/6-31G algorithm. The equilibrium structures of the lowest-lying complexes were re-optimized through density functional theory (DFT) calculations, which were performed using the Gaussian 09 program package, MOPAC software, and ORCA 4.2.0.

A deeper insight into weak interactions among complexes was acquired through the independent gradient model (Lefebvre et al., 2017) with the help of the Multiwfn program (version 3.3.9) (Lu and Chen, 2012) and visualized using VMD software (version 1.9.3). The theoretical Gibbs free energy ($\Delta G_{theoretical}$) for the copigmentation reaction was determined according to Eq. (5):

$$\Delta G_{theoretical} = G_{complex} - G_{copigment} - G_{anthocyanin} \quad (5)$$

where $G_{complex}$, $G_{copigment}$, and $G_{anthocyanin}$ denote the Gibbs free energies of the reaction complex, copigment, and anthocyanin, respectively.

2.7. Statistical analysis

Each experiment was repeated three times. SPSS 25 software was used for statistical analysis of the data at a significance level of $P \leq 0.05$. The differences between the average values for each treatment was obtained using an ANOVA Tukey test.

3. Results and discussion

3.1. Identification of anthocyanins

The molecular ions, fragment ions, and retention times of the anthocyanins for UHPLC-MS are listed in Table 1. The anthocyanins were identified by the major aglycone ions at m/z 301 (peonidin), 271 (pelargonidin), 331 (malvidin), 287 (cyanidin), and 317 (petunidin), consistent with the results of previous reports (Gutiérrez-Quequezana et al., 2020). Various anthocyanins were formed by combinations of aglycones with different types of glycosyl groups. The extract contained four peonidin, one pelargonidin, three malvidin, one cyanidin, and one petunidin derivative, with different proportions of each. PCG was the most abundant anthocyanin, accounting for 51.39% of the total anthocyanin content in both the dried potatoes. Most of the anthocyanins in PSA were acylated, consistent with the results of previous studies (Niu et al., 2021). Establishing specific anthocyanin structures and their relative contents in PSA provided us with a foundation for analyzing the effect of each organic acid on the stability of the colored complex.

3.2. Color changes due to anthocyanins copigmentation

One factor affecting the copigmentation reaction is the PSA:copigment molar ratio. The compounds produced by complexation of the flavylium cations of PSA with the copigments would shift the reaction equilibrium to favor the formation of flavylium ions, and hence the copigmented solutions exhibited a hyperchromic shift, i.e., an increase in the intensity of the absorbance maximum, ΔA_{max}. Additionally, a bathochromic shift, i.e., a shift to a longer wavelength $\Delta\lambda_{max}$, has been observed in response to copigmentation (Ghareaghajlou et al., 2021). Fig. 2(a)-(e) show that copigmentation resulted in increased absorbance in the range of 400–700 nm, indicating a hyperchromic effect for each type of copigments, the magnitude of which was dependent on the molar ratio. However, a significant difference not observed between the absorbance of the natural PSA at λ = 527 nm before and after the

Table 1
PSA extract content.

	Anthocyanins	Retention time (min)	Observed $[M]^+$ (m/z)	Theoretical $[M]^+$ (m/z)	Mass error (ppm)	Fragment ions (m/z)	Relative contents (%)
1	Peonidin-3-caffeoyl sophoroside-5-glucoside	5.239	949.2628	949.2608	2.1069	787, 463, 301	8.27 ± 1.53
2	Pelargonidin-3-feruloyl rutinoside-5-glucoside	5.244	917.2751	917.2710	4.4698	755, 433, 271	8.95 ± 0.84
3	Malvidin-3-caffeoyl rutinoside-glucoside	5.345	801.2248	801.2237	1.3729	493, 331	8.51 ± 0.61
4	Peonidin-3-caffeoyl rutinoside-5-glucoside	5.349	933.2601	933.2659	−6.2147	771, 463, 301	8.50 ± 1.76
5	Malvidin-3-caffeoyl rutinoside-5-glucoside	5.365	963.2725	963.2765	−4.1525	801, 493, 331	20.89 ± 3.65
6	Cyanidin-3-O-rutinoside	5.570	595.1633	595.1657	−4.0324	449, 287	14.38 ± 3.89
7	Peonidin-3-coumaroyl-5-glucoside	6.073	609.1605	609.1602	0.4925	463, 301	3.72 ± 0.28
8	Petunidin-3-coumaroyl rutinoside-5-glucoside	6.254	933.2594	933.2659	−6.9219	711, 479, 317	51.39 ± 4.48
9	Peonidin-3-coumaroyl rutinoside-5-glucoside	6.490	917.2681	917.2710	−3.1616	755, 463, 301	23.85 ± 2.83
10	Malvidin-3-coumaroyl rutinoside-5-glucoside	6.528	947.2837	947.2816	2.2169	785, 493, 331	6.08 ± 0.45

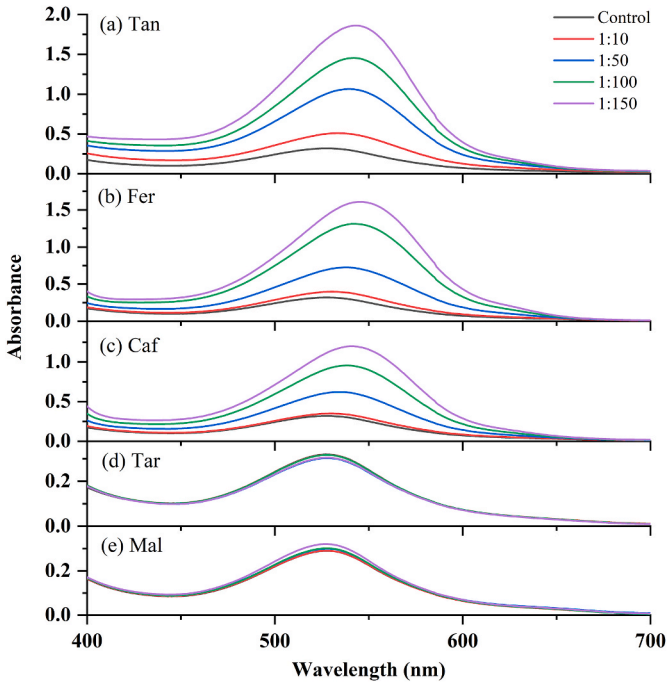

Fig. 2. Visible spectra of PSA (control) and PSA-copigments complexes with various PSA:copigments molar ratios ((a)–(e)).

addition of different concentrations of Tar or Mal (Fig. 3). In contrast with the other acids, Mal and Tar do not have structures that include phenol rings. According to previous studies (Sun et al., 2010), π-π interactions are the driving force for the strong intermolecular copigmentation between anthocyanins and phenol rings.

As shown in Fig. 3(a) and (b), the addition of copigments at molar ratios in the range of 1:10–1:150 increased the wavelength by 0–17.66 nm and changed the absorbance by between −5.22% and 482.99%. For each copigment used, the lowest and highest hyperchromic shifts among the copigmented complex solutions were observed for PSA:copigment molar ratios of 1:10 and 1:150, respectively. Kanha et al. reported that among three anthocyanins:copigments molar ratios-1:1, 1:10, and 1:100-tested in a study of anthocyanins copigmentation with Fer, dopamine, (+)-catechin, and cyanidin-3-O-glucoside, the highest molar ratio was associated with the highest $\Delta\lambda_{max}$ and ΔA_{max} (Kanha et al., 2019). This result could be attributed to the fact that the more copigments added to anthocyanins, the more complexes will be synthesized. This enhances the red color of the solution, thus increasing the absorbance of flavylium form. However, our results indicated that the molar concentration could not be increased indefinitely; after 24 h, flocculation had occurred in the 1:150 solution, which might have been a result of the addition of excess acid. Therefore, we used the solution with a molar ratio of 1:100 for thermal-stability testing.

Among the five copigments analyzed, the highest values of $\Delta\lambda_{max}$ and ΔA_{max} were observed for copigmentation of PSA with Tan, followed by Fer, Caf, Tar, and Mal, in order. In Fig. 4, the HOMO-LUMO energy gap ΔE (the energy required to promote an electron from the HOMO to the LUMO) is shown for each of the five acids. ΔE can also be used as a

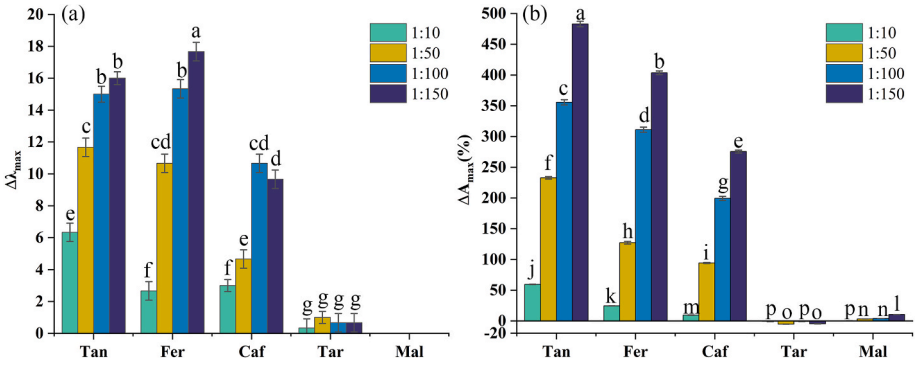

Fig. 3. Effect of intermolecular copigmentation on PSA absorption spectrum: (a) bathochromic shifts and (b) hyperchromic effects. According to the ANOVA Tukey test, the same letters above indicate not significant differences; ($P \leq 0.05$).

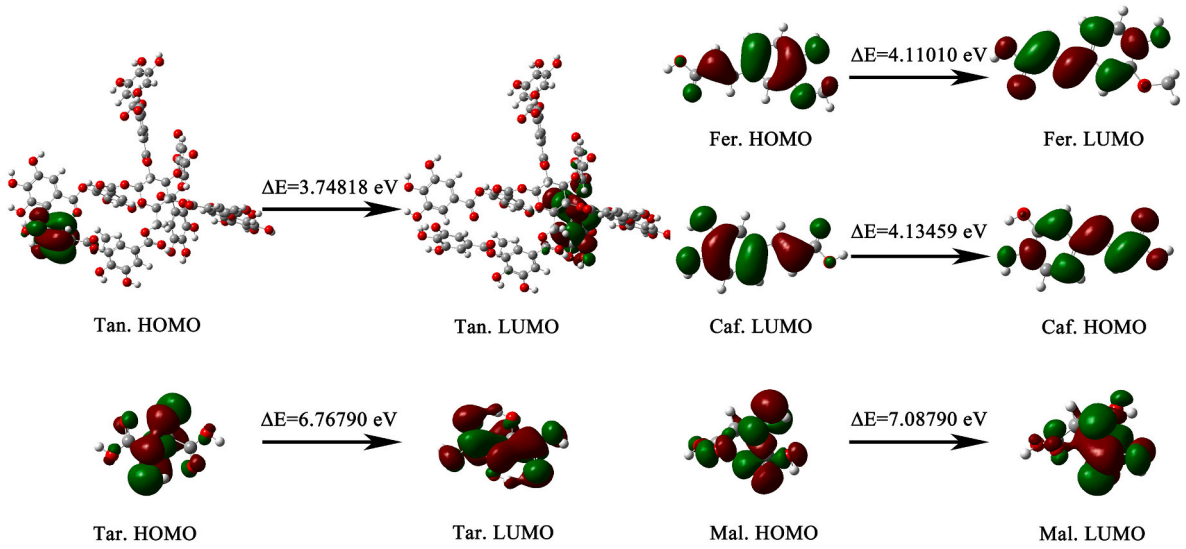

Fig. 4. Optimized structures, HOMOs, LUMOs, and HOMO-LUMO energy gaps ΔE of five acids calculated using DFT.

measure of the ability of the acid to lose or share electrons. It was found that the smaller the value of ΔE, the more readily copigmentation with PSA occurred. Therefore, we speculated that the values of ΔE could be used as a preliminary guide to the relative copigmentation capabilities of the acids. Indeed, the differences among the values of $\Delta\lambda_{max}$ and ΔA_{max} for the different acids were obviously correlated with the structures of the acids. More noncovalent interactions existed between copigments with more hydroxy groups and anthocyanins. Compared to the other acids, Tan had a greater number of hydroxy groups; therefore, larger $\Delta\lambda_{max}$ and ΔA_{max} were observed for its copigmentation with PSA. The hydroxycinnamic acids Fer and Caf have C_6–C_3 structures. A methoxy group on the aromatic ring may cause delocalization of the π electrons in the copigments, strengthening the π-π interactions between the phenol groups and anthocyanins aromatic rings. Therefore, compared with Caf, the copigmentation of Fer with PSA resulted in greater $\Delta\lambda_{max}$ and ΔA_{max} values. Tar and Mal did not possess methyl groups or aromatic rings. In summary, the phenolic acids had stronger copigmentation effects than the fatty acids. The π-π interactions between phenolic aromatic rings and anthocyanins are expected to be strong, which explains the observed stability of the PSA-phenolic acids complexes, and should prevent hydration. In addition, more hydrogen bonds were formed between anthocyanins and copigments containing more

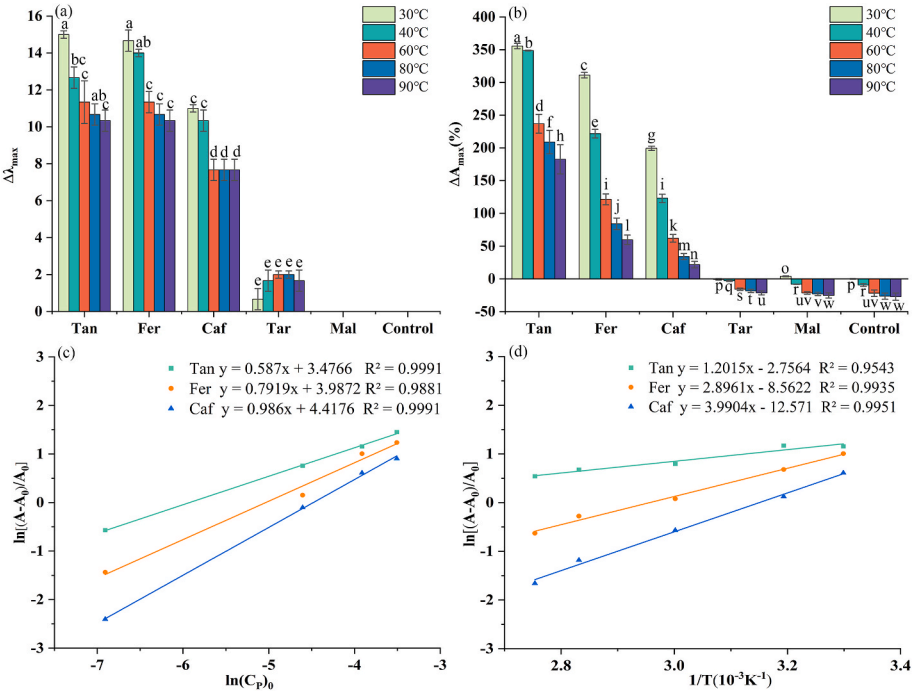

Fig. 5. Comparison of the influence of temperature during copigmentation on PSA (control) and copigmented-PSA for different copigments: (a) $\Delta\lambda_{max}$ and (b) ΔA_{max} (%) at different temperatures for the different acids. (c) Plots of $\ln[(A-A_0)/A_0]$ vs $\ln[C_p]_0$ for selected copigmentation reactions of PSA. (d) Plots of $\ln[(A-A_0)/A_0]$ vs reciprocal temperature (1/T) for selected copigmentation reactions of PSA. According to the ANOVA Tukey test, the same letters above indicate not significant differences; ($P \leq 0.05$).

methoxy or hydroxy groups (Sun et al., 2010). These mechanistic insights were validated by thermodynamic analyses and quantum mechanical calculations (see Sections 3.4 and 3.5).

3.3. Effect of temperature on copigmentation

The influence of temperature on copigmentation was investigated. As shown in Fig. 5(a) and (b), a shift in the maximum absorbance wavelength occurred toward lower wavelengths ($\Delta\lambda_{max}$), in each case except for the PSA-Tar and PSA-Mal complexes. Additionally, a progressive reduction in absorbance (ΔA_{max}) was observed when the temperature was increased from 30 to 90 °C, and the most significant change occurred at 90 °C. The increase in temperature shifted the equilibrium toward the reactants, destroying the weak interactions between the anthocyanins and copigments compounds. The values of ΔA_{max} indicated that increasing temperature was associated with a hypochromic effect. At 90 °C, the color intensity of the PSA-Tan copigmentation solution was reduced to 182.5%, whereas those of PSA-Fer and PSA-Caf were decreased to 59.73% and 21.83%, respectively. Although the absorbances of PSA-Tar and PSA-Mal treated at 40–90 °C were lower than that of the control group (PSA only) treated at 30 °C, these absorbances were higher than that of the control group treated at the same temperature; thus, degradation of these complexes occurred with increasing temperature, indicating that Tar and Mal did also effectively protect anthocyanins at lower temperatures. This result is consistent with the study of Molaeafard et al. (2021), in which the absorbances of complexes formed by the addition of Mal to anthocyanins at 100 °C were observed to be higher than that of natural anthocyanins at the same temperature but lower than that of natural anthocyanins at 20 °C. Zhang et al. (2009) also proved that the copigmentation of fatty acids (citric-acid monohydrate) increases the stability of PSA. In our study, anthocyanins formed the strongest and weakest copigmented complexes with Tan and Mal, respectively. These observations can also be linked to the chemical structures of the copigments; there were no phenol rings in Mal, and this structure contains and one hydroxy group less than Tar, but there were phenol rings and hydroxy groups in Tan. To further clarify the copigmentation mechanism, an investigation of the thermodynamic properties was performed, as described in the next section.

3.4. Determination of thermodynamic parameters

As shown in Fig. 5(c) and (d), plots of $\ln((A-A_0)/A_0)$ versus $\ln[C_p]_0$ and $1/T$ exhibited linear slopes with relatively high coefficients of determination ($R^2 > 0.95$). From the linear equations obtained, the thermodynamic parameters for the copigmentation reactions between PSA and the copigments were determined, using the slope and intercept of each curve according to the method described by Zhang et al. (2020). The equilibrium constant K indicates the strength of the binding between the copigments and anthocyanins, with a large K value correlating with a strong bond. Among the complexes we studied, the K value of the PSA-Caf complex was the highest, followed by those of the PSA-Fer and PSA-Tan complexes, as shown in Table 2. No parameters are reported in Table 2 for PSA-Tar and PSA-Mal because the absorbance of the complexes after the increase in temperature is lower than that of 30 °C blank group, as shown in Fig. 5(b). The value of n describes the relationship between the copigments and PSA. PSA-Caf exhibited an n value close to 1.0, indicating that the copigmentation between PSA and Caf shows a 1:1 correlation, consistent with a previous report by Xu et al. (2022).

The change in ΔG° was negative for each of the copigmentation complex formation reactions given in Table 2, indicating spontaneous reactions between PSA and these three copigments (Tan, Fer, and Caf). The highest-magnitude ΔG° value was calculated for PSA-Caf (−10.95 kJ/mol), followed by PSA-Fer (−9.88 kJ/mol), and PSA-Tan (−8.62 kJ/mol). Copigmentation involving hydroxycinnamic acids were found to be thermodynamically more favorable than those involving hydroxylation acids, indicating that Caf and Fer were the most efficient copigments, followed by Tan. The change in enthalpy ΔH° of the PSA copigmentation reaction was negative for each of the copigments, indicating that the reactions were exothermic.

Moreover, large bathochromic and hyperchromic shifts were observed within the temperature range of 30–40 °C, indicating the suitability of this temperature range for spontaneous exothermic reactions. The negative entropy, ΔS°, values indicated that copigmentation resulted in a loss of entropy and the formation of a more stable and ordered structure. The negative change in entropy also suggested that the anthocyanins and copigments were reorganized during complexation. This also indicated that the increase in entropy associated with the hydrophobic effect of complex formation did not compensate for the decrease in entropy caused by the loss, because of complexation, of rotational and translational degrees of freedom of the anthocyanins and copigments molecules (Nave et al., 2012). Among the PSA-acids interactions, the interaction between PSA and Caf resulted in the greatest loss of entropy, indicating the formation of a very compact complex with a high degree of order. The thermodynamic data on the copigmentation reactions indicated that van der Waals forces and hydrogen bonding were the main driving forces for copigmentation complex formation. This result was validated by quantum mechanical calculations.

Table 2
Thermodynamic parameters for the copigmentation reactions between PSA and selected copigments.

Copigmentation	K	n	ΔG° (kJ/mol)	ΔH° (kJ/mol)	ΔS° (kJ/mol)
PSA-Tan	32.35	0.59	−8.62	−4.88	−4.60
PSA-Fer	53.90	0.79	−9.88	−24.08	−47.61
PSA-Caf	82.90	0.99	−10.95	−33.18	−74.55

3.5. Quantum mechanical calculations

Theoretical calculations were performed to clarify the mechanism of copigmentation. Based on the observed hyperchromic effect and calculated thermodynamic parameters, Fer and PCG, the principal molecular component of PSA, were selected for quantum mechanical calculations. The DFT-optimized geometries of PCG, Fer, and the conformations of the copigmentation complexes of PCG and Fer were obtained, as shown in Fig. 6, where intermolecular hydrogen bonds are represented by green dotted lines. The PCG-Fer complex was found to exist in an arch-like conformation, possibly due to the steric hindrance caused by the acetyl group in PCG (Zhao et al., 2021). The theoretical value of Gibbs free energy of the complex was −42.27 (kcal mol^{-1}).

Weak interactions in the complex were investigated using an independent gradient model (IGM), to identify the regions and intensities of the interactions. In Fig. 6(d), a colorimetric scale is used for the isosurfaces: red indicates strong repulsive interactions, green indicates weak van der Waals forces, and blue indicates strong attractive interactions (hydrogen bonds and electrostatic interactions). All the complexes exhibited an extended green sheet-like region, mainly corresponding to π-π interactions. The hydroxy groups in Fer tended to form hydrogen bonds with PCG. The bond critical points (BCPs) listed in Fig. 6 can help distinguish the hydrogen bond (HBs) and van der Waals (vdWs) interaction. Ring critical points (RCPs) indicate the existence of ring structures, and cage critical points CCPs indicate that a cage is formed between several rings. Intermolecular CCPs and RCPs may indicate the existence of intermolecular π-π interactions and close contacts, respectively. Both these interactions were vdWs interactions. Therefore, together the HBs and vdWs bonds were the main driving force for the formation of the copigmentation complexes, confirming the conclusions drawn from the thermodynamics experiments.

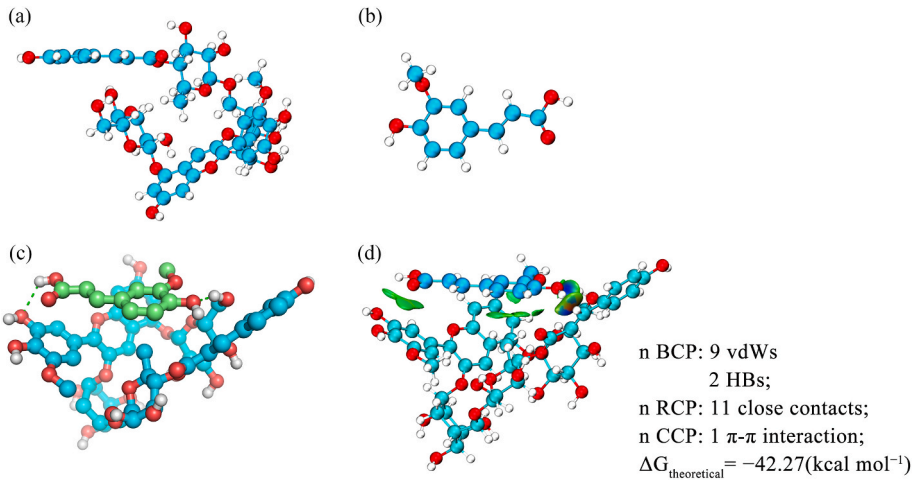

Fig. 6. Optimized geometries of (a) PCG and (b) Fer. (c) Hydrogen bonds in PCG-Fer complex. (d) Weak interactions between PCG and Fer after optimization.

4. Conclusions

In this study, measurements revealed that PCG was the principal ingredient of PSA. The addition of natural phenolic acids (Tan, Fer, and Caf) to PSA significantly increased its color intensity, with 1:100 being the optimum PSA:acid molar ratio. For Tan, the minimized HOMO-LUMO energy gap, the existence of several hydroxy groups, and the presence of several phenol rings within its structure explained its strong noncovalent intermolecular π-π interactions with PSA. Moreover, Tar and Mal induced the lowest number of copigmentation changes, in stark contrast to the aromatic acids, due to the absence of a phenolic ring in their structures. The protective effect of fatty acids on anthocyanins was weaker than that of phenolic acids under heating conditions. Thermodynamic data indicated that the enthalpy change for complex formation was most negative for PSA-Caf; this complex also exhibited the highest equilibrium constant. Furthermore, quantum mechanical calculations confirmed that noncovalent interactions (vdWs and HBs) were the main driving forces of copigmentation. Thus, this study provides a theoretical basis for the use of anthocyanins as food colorants.

Funding

This research was supported by Natural Science Funds of Hebei Province of China [grant number C2020204123], the Young Scholar Scientific Reuter Foundation of Hebei Agricultural University [grant number YJ201946] and the Research of Key Technologies and Development of Product for Comprehensive Utilization of Potato [grant number 20327103D].

CRediT authorship contribution statement

Xiaorui Lv: Investigation, Writing – original draft. **Jianlou Mu:** Writing – original draft. **Wenxiu Wang:** Methodology. **Yaqiong Liu:** Conceptualization. **Xiaomin Lu:** Data curation. **Jianfeng Sun:** Project administration. **Jie Wang:** Validation. **Qianyun Ma:** Writing – review & editing.

Declaration of competing interest

The authors declare that they have no known competing financial interests or personal relationships that could have appeared to influence the work reported in this paper.

References

Alara, O.R., Abdurahman, N.H., Ukaegbu, C.I., 2021. Extraction of phenolic compounds: a review. Curr. Res Food Sci. 4, 200–214. https://doi.org/10.1016/j.crfs.2021.03.011.

Aleixandre-Tudó, J.L., Alvarez, I., Lizama, V., García, M.J., Aleixandre, J.L., Du Toit, W. J., 2013. Impact of caffeic acid addition on phenolic composition of Tempranillo wines from different winemaking techniques. J. Agric. Food Chem. 61, 11900–11912. https://doi.org/10.1021/jf402713d.

Amchova, P., Kotolova, H., Ruda-Kucerova, J., 2015. Health safety issues of synthetic food colorants. Regul. Toxicol. Pharmacol. 73, 914–922. https://doi.org/10.1016/j.yrtph.2015.09.026.

Babaloo, F., Jamei, R., 2018. Anthocyanin pigment stability of Cornus mas-Macrocarpa under treatment with pH and some organic acids. Food Sci. Nutr. 6, 168–173. https://doi.org/10.1002/fsn3.542.

Cai, D., Li, X., Chen, J., Jiang, X., Ma, X., Sun, J., Tian, L., Vidyarthi, S.K., Xu, J., Pan, Z., Bai, W., 2022. A comprehensive review on innovative and advanced stabilization approaches of anthocyanin by modifying structure and controlling environmental factors. Food Chem. 366, 130611 https://doi.org/10.1016/j.foodchem.2021.130611.

Choi, Y.E., Choi, S.I., Han, X., Men, X., Jang, G.W., Kwon, H.Y., Kang, S.R., Han, J.S., Lee, O.H., 2020. Radical scavenging-linked anti-adipogenic activity of Aster scaber ethanolic extract and its bioactive compound. Antioxidants 9. https://doi.org/10.3390/antiox9121290.

Fan, L., Wang, Y., Xie, P., Zhang, L., Li, Y., Zhou, J.J.F.C., 2019. Copigmentation effects of phenolics on color enhancement and stability of blackberry wine residue anthocyanins: chromaticity, kinetics and structural simulation. Food Chem. 275, 299–308. https://doi.org/10.1016/j.foodchem.2018.09.103.

Fenger, J.-A., Roux, H., Robbins, R.J., Collins, T.M., Dangles, O., 2021. The influence of phenolic acyl groups on the color of purple sweet potato anthocyanins and their metal complexes. Dyes Pigments 185. https://doi.org/10.1016/j.dyepig.2020.108792.

Gençdağ, E., Özdemir, E.E., Demirci, K., Görgüç, A., Yılmaz, F.M., 2022. Copigmentation and stabilization of anthocyanins using organic molecules and encapsulation techniques. Curr. Plant Biol. 29 https://doi.org/10.1016/j.cpb.2022.100238.

Ghareaghajlou, N., Hallaj-Nezhadi, S., Ghasempour, Z., 2021. Red cabbage anthocyanins: stability, extraction, biological activities and applications in food systems. Food Chem. 365, 130482 https://doi.org/10.1016/j.foodchem.2021.130482.

Gutiérrez-Quequezana, L., Vuorinen, A.L., Kallio, H., Yang, B., 2020. Impact of cultivar, growth temperature and developmental stage on phenolic compounds and ascorbic acid in purple and yellow potato tubers. Food Chem. 326, 126966 https://doi.org/10.1016/j.foodchem.2020.126966.

He, B., Zhang, L.L., Yue, X.Y., Liang, J., Jiang, J., Gao, X.L., Yue, P.X., 2016. Optimization of Ultrasound-Assisted Extraction of phenolic compounds and anthocyanins from blueberry (Vaccinium ashei) wine pomace. Food Chem. 204, 70–76. https://doi.org/10.1016/j.foodchem.2016.02.094.

He, X.-l., Li, X.-l., Lv, Y.-p., He, Q., 2015. Composition and color stability of anthocyanin-based extract from purple sweet potato. Food Sci. Technol. 35, 468–473. https://doi.org/10.1590/1678-457X.6687.

Huang, Y., Zhou, S., Zhao, G., Ye, F., 2021. Destabilisation and stabilisation of anthocyanins in purple-fleshed sweet potatoes: a review. Trends Food Sci. Technol. 116, 1141–1154. https://doi.org/10.1016/j.tifs.2021.09.013.

Kanha, N., Surawang, S., Pitchakarn, P., Regenstein, J.M., Laokuldilok, T., 2019. Copigmentation of cyanidin 3-O-glucoside with phenolics: thermodynamic data and thermal stability. Food Biosci. 30 https://doi.org/10.1016/j.fbio.2019.100419.

Lefebvre, C., Rubez, G., Khartabil, H., Boisson, J.-C., Contreras-García, J., Hénon, E., 2017. Accurately extracting the signature of intermolecular interactions present in

the NCI plot of the reduced density gradient versus electron density. Phys. Chem. Chem. Phys. 19 (27), 17928–17936. https://doi.org/10.1039/C7CP02110K.
Liu, J., Huang, J., Ying, Y., Hu, L., Hu, Y., 2021. pH-sensitive and antibacterial films developed by incorporating anthocyanins extracted from purple potato or roselle into chitosan/polyvinyl alcohol/Nano-ZnO matrix: comparative study. Int. J. Biol. Macromol. 178, 104–112. https://doi.org/10.1016/j.ijbiomac.2021.02.115.
Lu, T.. Molclus program, version 1.5. http://www.keinsci.com/research/molclus.html. (Accessed 20 March 2021).
Lu, T., Chen, F., 2012. Multiwfn: a multifunctional wavefunction analyzer. J. Comput. Chem. 33 (5), 580–592. https://doi.org/10.1002/jcc.v33.510.1002/jcc.22885.
Molaeafard, S., Jamei, R., Poursattar Marjani, A., 2021. Co-pigmentation of anthocyanins extracted from sour cherry (Prunus cerasus L.) with some organic acids: color intensity, thermal stability, and thermodynamic parameters. Food Chem. 339, 128070 https://doi.org/10.1016/j.foodchem.2020.128070.
Nave, F., Brás, N.F., Cruz, L., Teixeira, N., Mateus, N., Ramos, M.J., Di Meo, F., Trouillas, P., Dangles, O., De Freitas, V., 2012. Influence of a flavan-3-ol substituent on the affinity of anthocyanins (pigments) toward vinylcatechin dimers and proanthocyanidins (copigments). J. Phys. Chem. B 116, 14089–14099. https://doi.org/10.1021/jp307782y.
Niu, X., Wang, W., Kitamura, Y., Wang, J., Sun, J., Ma, Q., 2021. Design and characterization of bio-amine responsive films enriched with colored potato (Black King Kong) anthocyanin for visual detecting pork freshness in cold storage. J. Food Meas. Char. 15, 4659–4668. https://doi.org/10.1007/s11694-021-01040-3.
Silva, M.M., Reboredo, F.H., Lidon, F.C., 2022. Food colour additives: a synoptical overview on their chemical properties, applications in food products, and health side effects. Foods 11. https://doi.org/10.3390/foods11030379.
Su, X., Griffin, J., Xu, J., Ouyang, P., Zhao, Z., Wang, W., 2019. Identification and quantification of anthocyanins in purple-fleshed sweet potato leaves. Heliyon 5, e01964. https://doi.org/10.1016/j.heliyon.2019.e01964.
Sun, J., Cao, X., Bai, w., Liao, X., Hu, X., 2010. Comparative analyses of copigmentation of cyanidin 3-glucoside and cyanidin 3-sophoroside from red raspberry fruits. Food Chem. 120, 1131–1137. https://doi.org/10.1016/j.foodchem.2009.11.031.
Tsuda, T., 2016. Recent progress in anti-obesity and anti-diabetes effect of berries. Antioxidants 5. https://doi.org/10.3390/antiox5020013.
Winter, A.N., Bickford, P.C., 2019. Anthocyanins and their metabolites as therapeutic agents for neurodegenerative disease. Antioxidants 8. https://doi.org/10.3390/antiox8090333.
Wu, J., Wang, X., He, Y., Li, J., Ma, K., Zhang, Y., Li, H., Yin, C., Zhang, Y., 2022. Stability evaluation of gardenia yellow pigment in presence of different phenolic compounds. Food Chem. 373, 131441 https://doi.org/10.1016/j.foodchem.2021.131441.
Xu, L., Yang, F., Dias, A.C.P., Zhang, X., 2022. Development of quantum dot-linked immunosorbent assay (QLISA) and ELISA for the detection of sunset yellow in foods and beverages. Food Chem. 385, 132648 https://doi.org/10.1016/j.foodchem.2022.132648.
Xu, Z., Wang, C., Yan, H., Zhao, Z., You, L., Ho, C.T., 2022. Influence of phenolic acids/aldehydes on color intensification of cyanidin-3-O-glucoside, the main anthocyanin in sugarcane (Saccharum officinarum L.). Food Chem. 373, 131396 https://doi.org/10.1016/j.foodchem.2021.131396.
Yang, J., Chen, J., Hao, Y., Liu, Y., 2021. Identification of the DPPH radical scavenging reaction adducts of ferulic acid and sinapic acid and their structure-antioxidant activity relationship. LWT 146. https://doi.org/10.1016/j.lwt.2021.111411.
Zhang, B., Wang, Q., Zhou, P.P., Li, N.N., Han, S.Y., 2020. Copigmentation evidence of oenin with phenolic compounds: a comparative study of spectrographic, thermodynamic and theoretical data. Food Chem. 313, 126163 https://doi.org/10.1016/j.foodchem.2020.126163.
Zhang, C., Ma, Y., Zhao, X., Mu, J., 2009. Influence of copigmentation on stability of anthocyanins from purple potato peel in both liquid state and solid state. J. Agric. Food Chem. 57, 9503–9508. https://doi.org/10.1021/jf901550u.
Zheng, J., Zheng, X., Zhao, L., Yi, J., Cai, S., 2021. Effects and interaction mechanism of soybean 7S and 11-S globulins on anthocyanin stability and antioxidant activity during in vitro simulated digestion. Curr. Res Food Sci. 4, 543–550. https://doi.org/10.1016/j.crfs.2021.08.003.